3D Smith Chart for plotting Rieke Diagrams of Microwave Oscillators

D Vishrutha, *Member, IEEE*, and Dr. Hemant Kumar., Senior *Member, IEEE*

***Abstract*—Rieke diagrams are an important load characteristic of microwave oscillators plotted on a Smith chart. It consists of two families of curves, one representing contours of constant power and the other contours of constant frequency. In oscillators such as magnetrons, the intersection of these two families of curves corresponds to point of operation corresponding to the locking signal frequency. An externally adjusted source determines the reflected power, so when the magnitude is increased and causes the magnitude of the reflection coefficient becomes greater than one. Since the reflection coefficient becomes greater than one it can no longer be plotted using the conventional Smith chart. A 3D Smith chart is a Riemann sphere-based Smith chart that allows plotting circuit parameters whose reflection coefficient magnitude is greater than unity hence overcoming the limitations of the conventional Smith chart. This paper discusses the methods of plotting Rieke diagrams of microwave oscillators on a 3D Smith chart using MATLAB.**

Index Terms*—Oscillators, Smith chart, Rieke diagrams, Riemann sphere

I. INTRODUCTION

A 3D Smith chart is a Riemann sphere-based Smith chart that permits circuit parameters with $|\Gamma| > 1$ to be shown, thereby bypassing the constraints of the standard Smith chart [1][2]. The 3D Smith chart allows for the plotting of any parameter that can be represented in terms of reflection coefficient, impedance, or admittance. A Rieke diagram is a representation of oscillator load characteristics on a Smith chart. A typical Rieke diagram consists of two families of curves, one representing contours of constant power and the other contours of constant frequency. According to [3], the frequency curves and power contours are roughly parallel to conductance and susceptance curves, respectively. [4] discusses how Rieke diagrams behave under various circumstances and entail intricate calculations of power and frequency contours using Bessel functions. The power contour equations in [5] are obtained based on the oscillator being in a free-running condition, and maximum power is assumed in order to normalize the power and keep the contours inside the unit circle. However, in the active stage, the behavior may change and cannot be normalized since the reflection is reliant on an externally controlled source and may extend outside the unit circle. Although the conventional Smith chart can be used for this, it only permits plotting for values $|\Gamma| < 1$, and any point outside the unit circle must be mapped back into the unit circle, which is not the case with the 3D Smith chart. The 3D Smith chart is a stereographic projection of the whole 2D conventional Smith chart, with $|\Gamma| < 1$, $|\Gamma| > 1$, and $|\Gamma| = 1$ mapped to the southern, northern, and equator, respectively

II. ANALYSIS OF POWER AND FREQUENCY CONTOURS

Although the peak power of the magnetron is stated in [7], some deviations in the power spectra have been noticed with regard to the reflection coefficient. The loss function of the Least mean square estimation (LMSE) approach has been presented to fit the experimental data from 2M244 Magnetron datasheets using regressional analysis [6]. The semi-empirical formulae were obtained using the condition that the minima of the loss function appear very close but greater than 1000W, which implies that the maximum power must be minimized. The physical postulate is that the power delivered reduces as the curves become distant from the point of peak power giving rise to an assumption that the contour curves represent an iso-centric model. Similarly, other parameters are identified by sampling the experimental data according to varying densities at different intervals of the curve.

The following equation is found for power contours:

$$P = a * \exp\left((b * ((\Gamma_r \cos(\theta) + \Gamma_i \sin(\theta)) - 0.22)^2 + c * ((\Gamma_r \sin(\theta) - \Gamma_i \cos(\theta)) - 0.026)^2\right) \quad (1)$$

Where, $\theta = 51.8418°$; $a = 1023$; $b = -0.4704$ and $c = -0.6252$, P −power, Γ_r – real part of reflection coefficient and Γ_i – imaginary part of reflection coefficient. The R-square is calculated under the Frobenius norm and is found to be 0.9893.

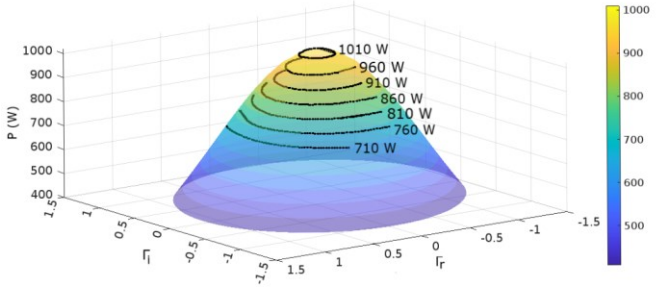

Fig. 1. Variation of Power with respect to the Rieke diagram

D Vishrutha graduated from NIT Trichy India on May 2022 and is currently working with the Antenna research group of Bharat Electronics Ltd. as a Design Engineer.

Dr. Hemant Kumar is an Assistant Professor at the ECE Department of NIT Trichy, India.

points i.e. reflection coefficient.

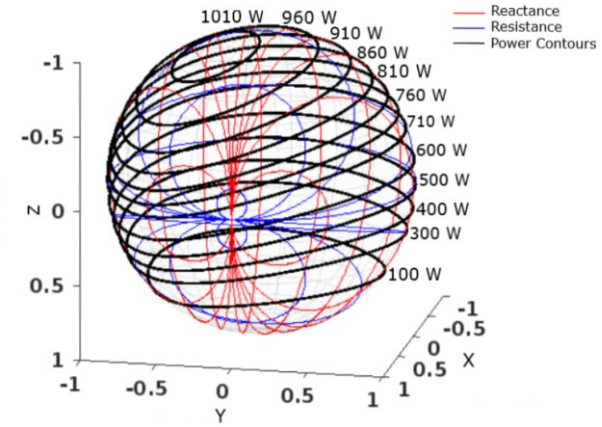

Fig. 2. Power contours mapped onto a 3D Smith chart using stereographic projection

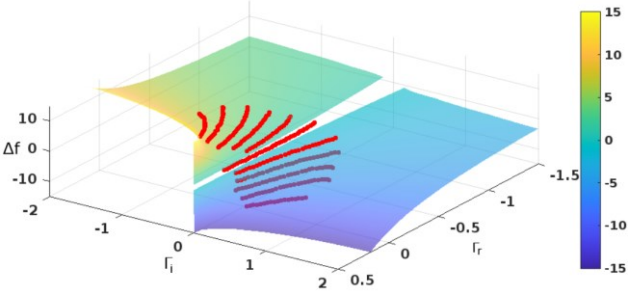

Fig. 3. Variation of frequency (Δf) in MHz with repect to the Rieke diagram points i.e. reflection coefficient overlayed with experimental data (red points).

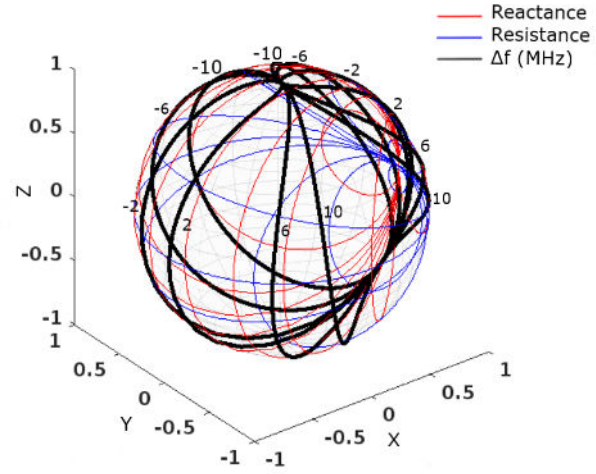

Fig. 4. Frequency contours mapped onto a 3D Smith chart using stereographic projection

The plot (Fig.3) only consists of the part of the conic section that fits the data. The vertical line corresponds to the apex of conic section for any value of Δf.
The frequency equation is found to be :

$$((\Gamma_r \cos(\theta) + \Gamma_i \sin(\theta)) - 0.48)^2 + \frac{\left((\Gamma_r \sin(\theta) - \Gamma_i \cos(\theta)) + \frac{1}{h(\Delta f)}\right)^2}{51.6} = \frac{1}{51.6}\left(\frac{1}{h(\Delta f)}\right)^2 \quad (2)$$

Where, $\theta = 8.115°$; $h(\Delta f) = -ln\left(1 + \frac{2.127\Delta f|\Delta f|}{2460}\right)$ and 2460 MHz is the resonant frequency.

The log is a natural choice as it maps the set of positive reals to the set of entire reals which coresspond to the extremities of susceptance loci (i.e. $\pm\infty$). Frequency contours behave similarly to susceptance loci in an admittance chart but with the extremes at 0 and ∞, additionally setting the center frequency a 2460 MHz. Any smooth function of interest can be well approximated using a power series expansion of this term.

V. Conclusion

Through performing regressional analysis on the experimental data, semi-empirical formulae have been found for power and frequency contours that fit the given region and asymptotic regions. A 3D Smith chart is used to plot these curves and it has been observed that it permits plotting of curves even when it goes out of the unit circle, which provides freedom of analysis of the behaviors outside and inside the unit circle as well. With more experimental data from different types of microwave oscillators, more generic and accurate empirical formulae may be found.

VI. Future Plans

We hope to obtain and analyze more experimental data and use it for further investigation into the device physics which will ultimately lead to better harness the usefulness of the device in regions that have not been of interest in the past. Also, the 3D Smith chart proves to be useful in analyzing the regions which cannot be analyzed using the conventional Smith chart. I am currently working in antenna field and would also like to work and explore the field of microwave electronic devices in future.

Acknowledgment

I would like to express my gratitude to my friends and family, Dr. S Raghavan, Dr. Lalit Kumar, Dr. B.N. Basu, Dr. Shivendra Maurya, delegates of VEDA'22 conference and MTTS for supporting, inspiring, and encouraging me to pursue a career in the field of microwave engineering. I graduated from NIT Trichy, India on May 2022 and am currently working with the Antenna research group of Bharat Electronics Ltd. Lastly, I would also like to thank Dr. Hemant Kumar for supporting me to apply for the MTTS Undergraduate scholarship awards.

References

[1] "Analyzing 3D Smith chart Using MATLAB: An Insightful And Illustrative Approach", D Vishrutha, Dr. Hemant Kumar, INCAP 2021.
[2] The 3D Smith chart from theory to experimental reality check, Andrei A. Muller, Victor Asavei, Alin Moldoveanu, Esther-Sanabria-Codesal, Riyaz A. Khadar4, Cornel Popescu, Dan Dascalu, Adrian. M. Ionescu, IEEE Microwave Magazine, vol 21, no 11, pp 22-35, Nov. 2020 (unedited). Available Online @ https://ieeexplore.ieee.org/document/9217562/
[3] E. E. David,Jr., "Locking phenomena in microwave oscillators", Technical report no. 63 April 8, 1948. Available Online @ https://dspace.mit.edu/bitstream/handle/1721.1/4985/RLE-TR-063-04706964.pdf?sequence=1&isAllowed=y
[4] D R. Hamilton, J. K. Knipp and J. B. H. Kuper, Klystron and Microwave Triodes, New York: McGraw-Hill, pp. 404-440, 1948
[5] K. Fukumoto, M. Nakajima and J. Ikenoue, "Mathematical Representation of Microwave Oscillator Characteristics by Use of the Rieke Diagram," in IEEE Transactions on Microwave Theory and Techniques, vol. 31, no. 11, pp. 954-959, Nov. 1983, doi: 10.1109/TMTT.1983.1131639.
[6] Bilik, Vladimir. (2019). Automatic Measurement of Magnetron Rieke Diagrams. 10.4995/AMPERE2019.2019.9782